Journal of Applied Polymer Science

Application of Shear Thickening Fluid in Ultra High Molecular Weight Polyethylene Fabric

Liang-Liang Sun, Dang-Sheng Xiong, Cai-Yun Xu
Department of Material Science and Engineering, Nanjing University of Science and Technology, Nanjing 210094, China
Correspondence to: D.-S. Xiong (E-mail: xiongds@163.com)

ABSTRACT: An advanced stab-resistant material composed of shear thickening fluid (STF) and ultra high molecular weight polyethylene (UHMWPE) fabric was investigated. STF was prepared by dispersing nanosilica (SiO_2) into ethylene glycol. The shear thickening behavior of STF with the increase of the shear rate was observed by PhysicaMCR301. STF/UHMWPE composite fabric was synthesized by impregnating UHMWPE fabric in STF dilution. Stab resistant experiment was conducted on a self-made stab test machine with knife and spike as stab tool. The results demonstrate that the stab resistant property of the UHMWPE fabric is greatly improved by impregnating STF. The stab resistant property is greatly increased with the increase of mass fraction of silica in STF. Especially, when the mass fraction of SiO_2 in STF is 38%, the stab resistance force and energy absorption of STF/UHMWPE are optimal for knife and spike threats. With the same stab resistant properties, the flexibility of UHMWPE fabric impregnated with STF is higher than that of the neat fabric. © 2013 Wiley Periodicals, Inc. J. Appl. Polym. Sci. 129: 1922–1928, 2013

KEYWORDS: composites; nanoparticles; nanowires and nanocrystals; textiles

Received 21 July 2012; accepted 19 November 2012; published online 3 January 2013
DOI: 10.1002/app.38844

INTRODUCTION

The traditional body armor materials was designed to protect the user from bullets attacks.[1] Because of the stringent gun control legislation, sharp instrument injury is far more than the bullet attacks. Considering the two kind of damage is different in the mechanism, a kind of new body armor needs to be studied. Liquid armor is a kind of stab resistant composite materials, which is composed of shear thickening fluid (STF) and fabric. STF exists in liquid form in the ordinary conditions. Once the fabrics start to get hit, STF turns into a very rigid solid-like material that prevents the threats from penetrating the soldier's body. When impact force is disappeared, STF is back to liquid form. Therefore, the shear response of the STF displays reversible transition and STF can be stable on the fabrics.[2,3] Personal body armor was used to protect the human body from the injury of the knife, dagger, and other sharp instrument.[4,5] During the puncture process, cone does not destroy the fabric so much and mostly pass through the fiber bundles. So the structure of the fabric has important influence on the stab-resistant property.[6] Termonia et al. established a model to analysis the factors, which influence the fabric performance.[7] Research shows that in multiply fabric systems, it can be found that the maximum force on the needle occurs during friction against its conical section after puncture by the tip has occurred. This type of body armor materials not only provide protection against sharp instrument threats, but also ensure its flexibility and proper comfort to make the user safe as well as not hindering them from moving. This means that the armor materials should be light and flexible, so it is necessary to seek a balance between the effective protective and flexibility.[8,9]

STF shows a non-Newtonian flow behavior, whose viscosity increases with the increase of shear rate or applied stress.[10–12] There are two microscopic mechanisms about shear thickening phenomenon: one is order–disorder transition, which was put forward by Hoffman, namely shear thinning is due to the rise of orderly degree of particles in the system and it is the same in reverse.[13,14] Another one is the "hydrocluster" mechanism, which was proposed by Brady, in which, shear thickening is thought to be induced by the "particle clusters" formed by flow force in the system, which finally leads to the viscosity increase of the system.[15–17] In the past few years, many researchers have used various methods to prepare the advanced stab-resistant material, which is composed of high performance fabric and STF.[18,19] Wanger et al. first impregnated Kevlar fabric with shear thickening, which composed of SiO_2/PEG200 to prepared advanced Body Armor and discussed the influence of varying amounts of SiO_2, patterns on the performance of materials.[15] Research showed that compared with neat Kevlar fabrics of equivalent weight, the STF-impregnated Kevlar fabric provided nearly the same ballistic protection yet was much thinner and more flexible.

Lee et al. demonstrated that energy absorption of the STF-fabric composite was proportional to the volume of STF.[20] Hassan et al. showed that STF impregnated both Kevlar and Nylon fabrics had better penetration resistance in dynamic stab test and the quasi-static loading compared with neat fabrics without affecting the fabric flexibility.[21] Considering the characteristics of ultra high molecular weight polyethylene (UHMWPE) fiber, because of high molecular weight, its impact resistance is four times higher than that of resistance of polycarbonate and wear resistance is several times higher than that of brass and carbon steel. The self-lubricating performance is excellent due to its small friction factor. However, there is no double bond and branch Chain in the molecular structure, the melting point of UHMWPE fiber is low, so UHMWPE fiber is more suitable for making stab-resistant material.[22–24]

UHMWPE fabric has great potential in body armor material due to its superior advantages. In this study, the STF was synthesized through the mechanical mixing method. STF/UHMWPE composite was prepared with static immersion method. Various targets are subjected to threat of knife and spike with dynamic loadings to evaluate the stab-resistant performance and energy absorption.[25,26]

EXPERIMENTAL

Materials

Tetraethoxysilane (TEOS) and ammonia solution, which were used to synthesize SiO_2 particles, were obtained from Shanghai LingFeng chemical reagent Company and Xilong Chemical Company, respectively. Ethylene glycol (EG) was used as the liquid polymer in the STF synthesis process and ethyl alcohol was used as the diluents. They were both supplied by Guangdong guanghua chemicals Plant Company. The UHMEPE fabric used in this study whose areal density is 120 g/m^2 and it was purchased from Jinhu Jeely Sport Product Company.

Synthesis

Preparation of Silica Particle. The silica particle was prepared by sol-gel method. Silica particle was prepared through hydrolysis of TEOS in ammonia solution. The dispersion medium was EG. Deionized water and absolute ethyl alcohol were added into a certain amount of the TEOS according to the proportion. The solution was put in the water-bath at 70°C and reacted for a period. Then ammonia water was added into the solution, and the reaction was continued for about 1 h until the gel was formed. The gel was then conducted by centrifuging and washing at room temperature. The colloid was dried in the vacuum drying oven for 24 h to remove ethyl alcohol. At last, the product was heated to 600°C for a period to get the pure silica powder.

Synthesis of STF

The STF was synthesized by mechanical mixing method, which is blending SiO_2 with EG using vortex hybrid device. SiO_2 particles was added into the EG slowly according to different weight percentage and mixing process was kept for several hours until SiO_2 powder was dispersed in the medium fluid uniformly. To improve the stability of the scattered system, the STF was put in the vacuum drying oven on 25°C and dried for about 24 h to remove the bubble during dispersed process.

Preparation of STF/UHMWPE Composite Fabric. The STF/UHMWPE composite fabric was prepared by impregnating process. Before impregnation, STF was diluted with ethanol to reduce the viscosity of the scattered system. UHMWPE fabrics were immersed in the STF/ethanol solution. The wet fabrics were squeezed using a 2-roll mangle to get rid of the excess amount of the solution and then the fabrics were put into the vacuum oven at 60°C for 1 h. At last, 8 layers of samples were sealed as a unit with polyethylene film for later use. Moreover, 8 layers of EG/UHMWPE composites were synthesized by impregnating fabrics with pure EG as a contrast. Each sample was tested three times at different regions of its surface.

Materials Testing and Characterization

The Analysis of Silica Particles. The phase analysis and functional group of silica powder were detected by the X-ray diffractometer (D8ADVANCE0, Germany) and FTIR (IR Prestige-21, Japan). The particle size of silica was measured by Laser particle size analyzer (Mastersizer2000e, Germany) with dry method. The surface morphology of silica powder and dispersion of STF in the fabric was observed by Scanning Electron Microscope. The STF/fabric composite and neat fabric samples were cut in to small pieces using the scalpel, and these two fabrics and silica powder were placed on a conductive tape and sprayed gold to ensure their conductivity.

The Rheological Properties Test of the STF. The rheological properties of the as-prepared STF with different weight percentage were tested by using PhysicaMCR301. Steady rheological property refers to the relationship between the viscosity η and shear rate γ. Testing was carried out at room temperature in a steady flowing mode in the shear rate range of 0–100 s^{-1} by using a rotator and a cone plate of size 25 mm and 1°angles.

Dynamic Stab Resistance Test. The stab resistant of neat fabric and STF/UHMWPE composite targets against spike and knife threats was evaluated by a homemade dynamic puncture tester based on NIJ standard.[27] Figure 1 shows the picture of the dynamic puncture tester configuration. The neat fabric was respectively 8 layers and 16 layers while EG/UHMWPE and STF/UHMWPE composites were 8 layers. Neat fabric and STF/fabric were cut into 150 × 150 mm^2 layers. The fabric targets were placed on the top of backing material, which consisted of four layers neoprene, one layer polyethylene bubble Plastic and two layers natural rubber. The drop height and weight of knife and spike threat is 0.6 m and 2.38 kg. To analyze the absorbed energy by the fabrics in Puncture process, the energy can be calculated from the penetration velocity and depth. We, respectively, defined the absorbed energy as E_1, E_2 (J) for knife and spike threats,

$$E_1 = \frac{1}{2} m_k \left({V_1}^2 - {V_2}^2 \right) \quad (1)$$

$$E_2 = \frac{1}{2} m_s \left({V_1'}^2 - {V_2'}^2 \right) \quad (2)$$

where m_k, m_s (kg) is the mass of knife and spike, V_1, $V_1^{'}$ (m s^{-1}) is the initial velocity of knife and spike, V_2, $V_2^{'}$ (m·s^{-1}) is the velocity after the impactors penetrate the targets. To relate the puncture depth with the residual velocity, a series of experiments

Applied Polymer SCIENCE

Figure 1. Homemade dynamic puncture tester. [Color figure can be viewed in the online issue, which is available at wileyonlinelibrary.com.]

have been carried out in the blank backing material. Figure 2 shows the linear relationship of the two factors about spike and knife threats.

Flexibility and Thickness Tests. To examine the effect of STF addition on the fabric flexibility, flexibility tests were performed for both neat fabric and STF/fabric composite samples by fabric bulging elastic tester. To measure the flexibility, neat fabric was prepared by stacking 8 layers and 16 layers and STF/UHMWPE composite was stacked 8 layers. The elastic recovery angle θ was measured and recorded for each specimen to examine the performance. Testing was carried out on the conditions that the pressure load is 10 N and pressurization time is 5 min ± 5 s. For the thickness test, a digital caliper was used to measure the specimen thickness.

RESULTS AND DISCUSSION

Structure of Silica Particles

Figure 3 shows the XRD spectrum of SiO_2 powder. It can be seen that amorphous diffraction peak appears in 20°–25°, which is the characteristic peak of silica. It is clear that the prepared SiO_2 powder is amorphous material. Figure 4 shows the FTIR spectrum of SiO_2 particles. At the wave number of 481 cm^{-1}, there is the bending vibration of Si—O—Si. The wave number of 790 and 1051 cm^{-1} are symmetric vibration and asymmetric vibration of Si—O. The wave number of 950 cm^{-1} is stretching vibration of Si—OH. The band at 1627 cm^{-1} is attributed to the vibration of O—H groups, which arise from the adsorption water by Si—OH.[28] Figure 5 shows the SEM images of SiO_2 powder. From the Figure 5, the SiO_2 particles are spherical and monodispersed. Combined with size distribution of silica particles in Figure 6, it can be seen that the average particle size of SiO_2 is about 500 nm.

Rheological Properties of STF

Figure 7 shows the curves of viscosity of the STF with different silica concentrations varied with shear rate. It can be concluded that the STF shows shear thinning behavior at the shear rate below critical values while it shows shear thickening behavior at high shear rates. Meanwhile, the viscosity of the disperse system increases with the increase of the content of silica. The thickening phenomenon is not very clear at lower content of silica. The decrease of solid particles in system results in weakness of the force between solid-liquid and decrease of viscosity. After shear thickening, hydrocluster becomes less and the flow resistance is reduced, so shear thickening behavior is not obvious. With the increase of mass fraction of silica, the critical shear rate reduces gradually. The main reason is that the viscosity increases with the concentration of the silica in EG, hydroclusters can be formed more easily and shear thickening behavior occurred with lower shear forces.

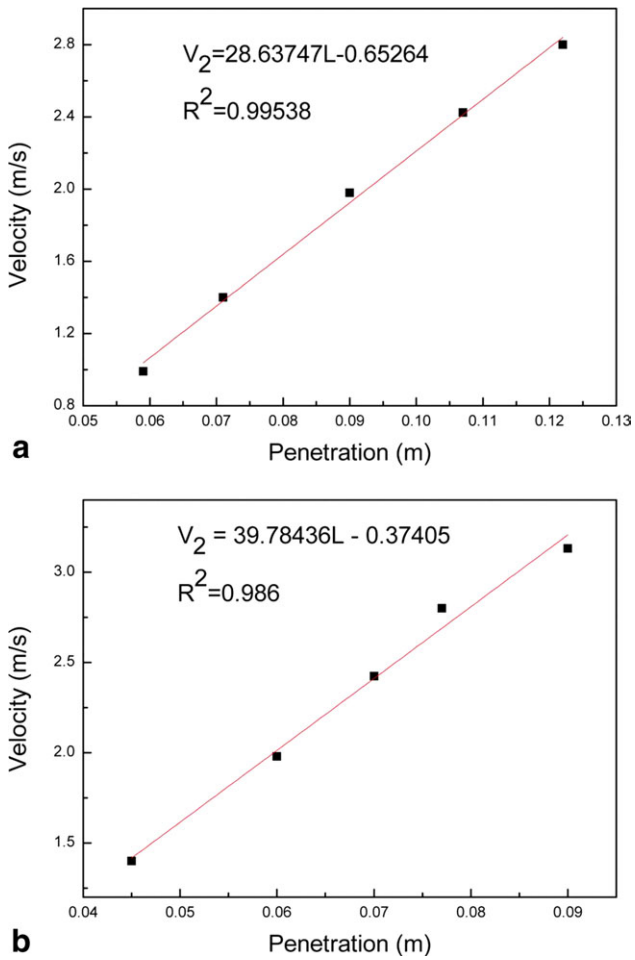

Figure 2. The relationship between the penetration depth and velocity in the blank backing material for spike (a) and knife (b). [Color figure can be viewed in the online issue, which is available at wileyonlinelibrary.com.]

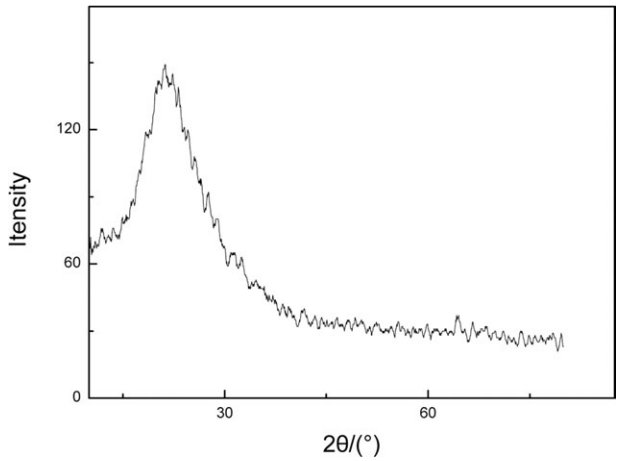

Figure 3. XRD spectrum of SiO_2 powders.

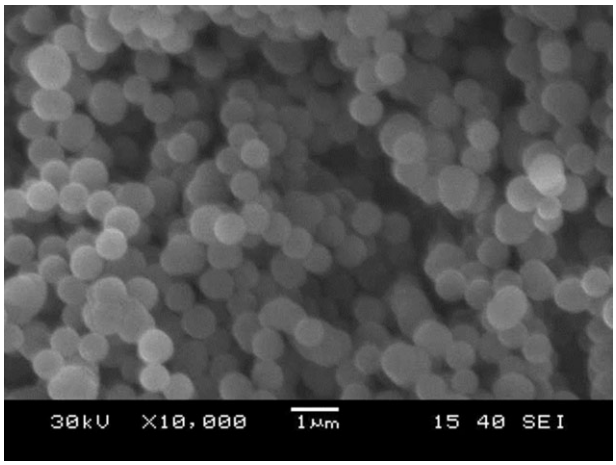

Figure 5. SEM images of SiO_2 powders.

Micrographs of STF/UHMWPE Composite

Figure 8(a–d) shows SEM images of neat UHMWPE fabrics and STF/UHMWPE composite at different magnifications. Figure 8(a) is the SEM image of neat UHMWPE fabrics, and it can be seen that UHMWPE fabric was woven by the fiber and there is a space between the fiber bundles. Figure 8(b) shows SEM image of STF/UHMWPE composite and STF is evenly distributed on the UHMWPE fabric. Figure 8(c) clearly presents that SEM image of STF/UHMWPE composite at ×500, the gap between the fabric bundles is filled with STF. The high magnification SEM image presented in Figure 8(d) shows that SiO_2 is completely dispersed between the UHMWPE fibers and a section of SiO_2 is reunited in the dispersion medium. These images indicate that the STF is well dispersed in UHMWPE fabric.

Dynamic Stab Performance

Stab Resistant Performance of Different Quality Fraction. Figure 9 shows the stab resistance force of the neat fabric, EG/UHMWPE and STF/UHMWPE composites with different mass fractions of SiO_2 in STF for knife and spike threats, whose drop height is 0.6 m. As seen in Figure 9, with the increase of mass fraction of silicon powder in STF, the stab resistance of STF/UHMWPE composite increases under threats of knife or spike.

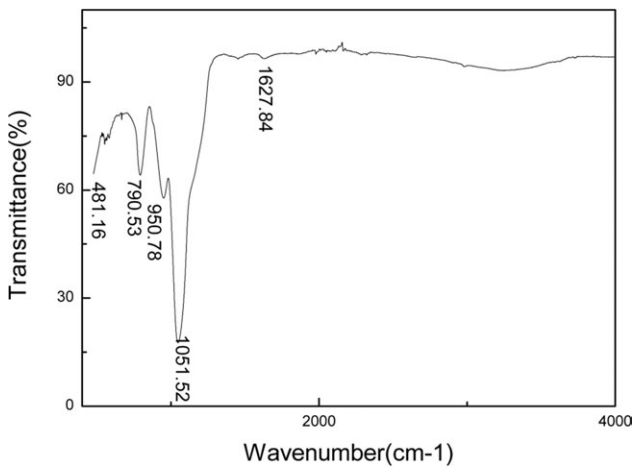

Figure 4. FTIR spectrum of SiO_2 particles.

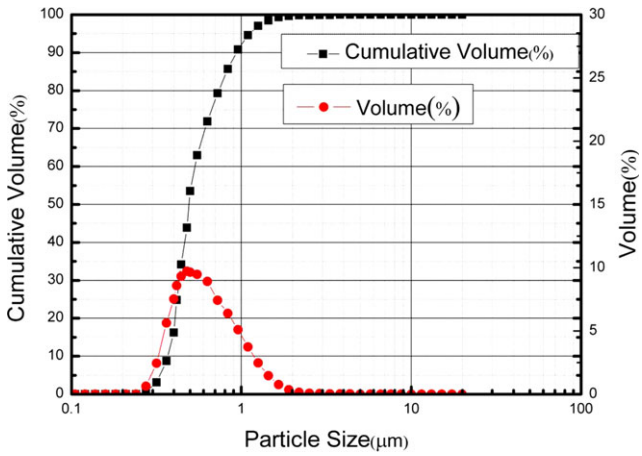

Figure 6. Size distribution of silica particles. [Color figure can be viewed in the online issue, which is available at wileyonlinelibrary.com.]

For the spike threat, with mass fraction of nanoparticle in STF of 38%, the force of 8 layers STF/UHMWPE composite is dramatically improved compared with 8 layers neat fabric, which is comparable with that of 16 layers neat fabric. Yet, the weight of

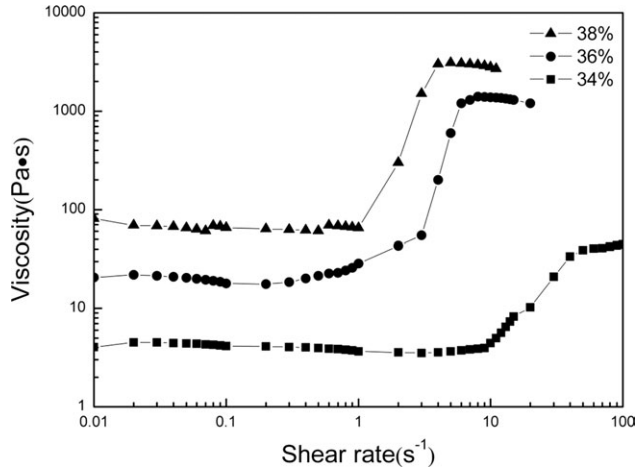

Figure 7. The rheological curve of STF suspensions at different SiO_2 mass fraction.

Applied Polymer SCIENCE

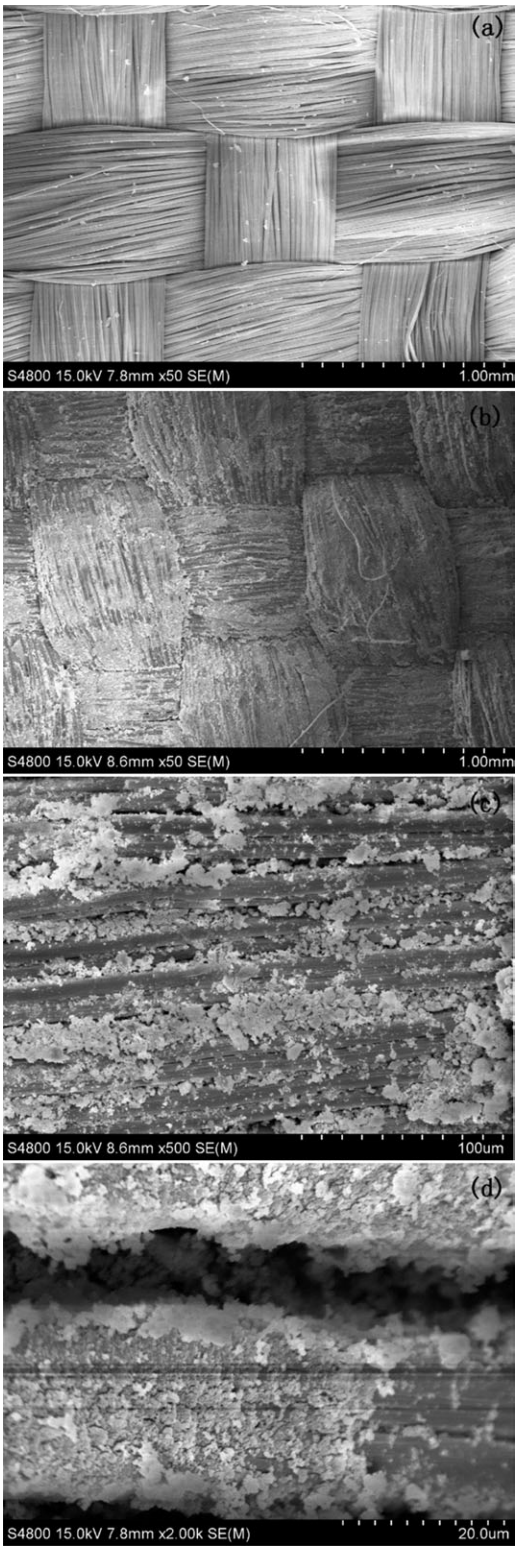

Figure 8. SEM images of neat UHMWPE fabric (a) and STF/UHMWPE composite (b–d).

composite with 8 layers is lower than that of the neat fabric with16 layers. By impregnating fabrics with STF, the compactness of the fabric structures is increased and the movement of the fiber bundles is limited. Under high-speed impact, the particles in the STF quickly gather together. Spike cannot easily push away the fiber bundles and the action of spike across the bundles of fabric is restricted. Although the force of EG/UHMWPE fabric is moderate, the fabrics are damaged and completely penetrated.

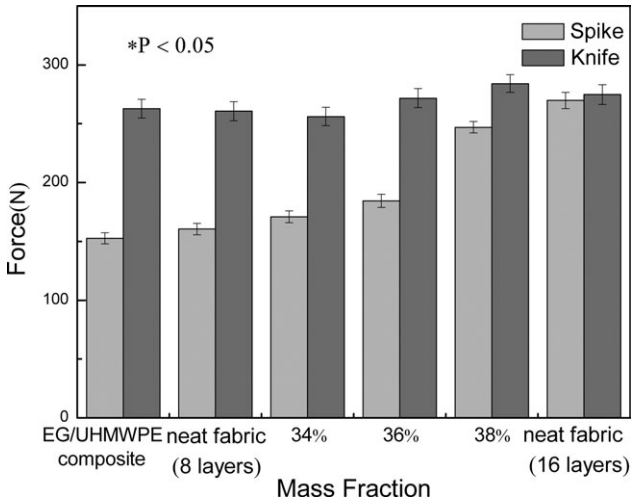

Figure 9. Stab resistance force of STF/UHMWPE composite with different mass fraction of SiO_2 in STF and neat fabric for spike and knife threats.

Compared with spike threat, the stab resistance under knife threat is less improved on STF/UHMWPE composite. It is probably concluded that during the puncture process, the tools mainly effect on the fabric by cutting the fiber. However, STF improves the compactness of the fabric instead of breaking strength of fiber. Under knife threat, the breaking strength of fiber is less affected by STF and the cutting resistance of fabric is not improved, so there is no significant difference among neat fabric, EG/UHMWPE and STF/UHMWPE composites.

Energy Absorption of Neat Fabric and STF/UHMWPE Composite. The penetration depth of neat fabric, EG/UHMWPE and STF/UHMWPE composites for knife and spike threats are presented in Tables I and II. According to formula (1) and (2), absorption energy of the targets can be calculated. With the increase of mass fraction of silica, the penetration depth decreases. The penetration depth of EG/UHMWPE composite is the highest among all the targets.

Table I. The Penetration Depth of STF/UHMWPE Composite and Neat Fabric for Knife Threat

Target	Neat fabric		EG			
	8 layers	16 layers	0	34%	36%	38%
Penetration depth (mm)	53.7	51.2	60.2	57.4	48.3	43.8
	55.1	50.4	60.4	58.9	48.1	45.4
	56.4	49.7	59.6	60.1	48.5	45.1
STDEV	1.35	0.75	0.42	1.35	0.2	0.85

Table II. The Penetration Depth of STF/UHMWPE Composite and Neat Fabric for Spike Threat

Target	Neat fabric		EG			
	8 layers	16 layers	0	34 %	36 %	38 %
Penetration depth (mm)	117.9	90.4	137.8	116.2	107.7	98.9
	120.1	89.7	140.1	115.6	109.5	100.1
	119.5	91.2	139.5	115.4	110.0	100.3
STDEV	1.14	0.75	1.19	0.42	1.21	0.76

Figure 10 shows the absorption energy of neat fabric, EG/UHMWPE and STF/UHMWPE composites for the knife and spike threats. For spike threat, the energy absorption by the STF-fabric composite is found to be proportional to the mass fraction of silica in STF. It is likely to be because STF absorbs most of gravitational potential energy during the puncture process and energy absorption of STF plays a primary role.

For knife threat, the penetration energy of STF/UHMWPE composite targets, however, is slightly more than the neat fabric target and EG/UHMWPE composite. The fabrics are damaged and completely penetrated during the puncture process. The conclusion is that it might be related with the effect of knife on fiber. The gravitational potential energy is mostly translated into internal energy. It can be seen from Figure 10 that absorption energy of EG/UNMWPE composite is the lowest for the knife and spike threats. The poor performance of the EG/UHMWPE targets may result from the lubricating effect of the EG. The friction between fibers is reduced during the puncturing process. The STF/UHMWPE composite targets exhibit superior stab resistance performance compared with the neat UHMWPE fabric and EG/UHMWPE composite targets.

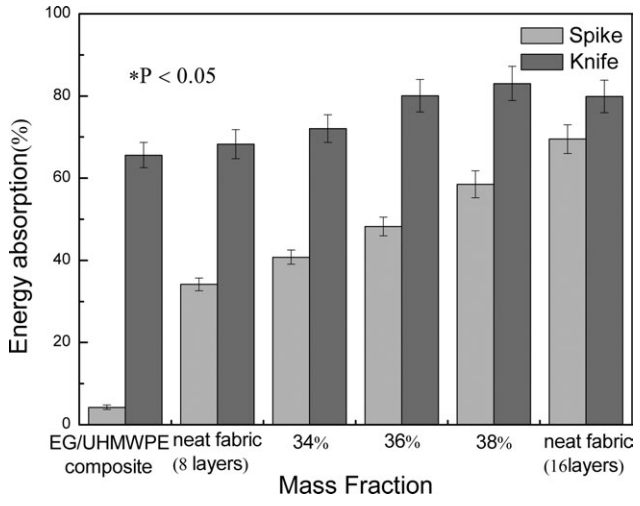

Figure 10. The absorption energy of STF/UHMWPE composite with different mass fraction of SiO_2 in STF and neat fabric for spike and knife threats.

Table III. Flexibility and Thickness for Neat Fabric and STF/UHMWPE Composite Fabric

Sample	Number of layers	Sample weight (g)	Recovery angle (°)	Sample thickness (mm)
Neat UHMWPE fabric	8	21.5 ± 0.8	33 ± 0.3	1.78 ± 0.21
Neat UHMWPE fabric	16	42.5 ± 0.7	17 ± 0.3	3.6 ± 0.19
STF/UHMWPE composite	8	26.6 ± 0.8	30.5 ± 0.5	2.31 ± 0.15

Flexibility and Thickness for Neat r Fabric and STF/UHMWPE Composite Fabric. Table III shows the results of flexibility and thickness test for 8 and 16 layers of neat fabric, and 8 layers of STF/UHMWPE composite. This results show that the addition of STF causes no change in the thickness and flexibility of UHMWPE fabrics.

The flexibility of 8 layers of STF/UHMWPE composite is better than that of 16 layers neat fabric, although the stab resistance forces of 8 layers of STF/UHMWPE composite and 16 layers neat fabric are similar. In conclusion, the STF/fabric composites exhibit better stab resistance and good flexibility compared with neat fabric targets.

CONCLUSIONS

The monodispersed SiO_2 particles with average particle size of about 500 nm were hydrolytic synthesized by sol-gel method. STF was prepared by mixing nanoparticles with EG. With the increase of mass fraction of silicon, the initial and the maximum viscosities of the system increase and the critical shear rate decreases.

The STF/UHMWPE composite fabric was prepared by impregnating UHMWPE fabric with STF. The gap between fiber bundles is filled by STF and STF is uniformly distributed in UHMWPE fabrics. The STF/UHMWPE composite target with 8 layers and the mass fraction of silicon in STF of 38% is comparable with that of the neat UHMWPE fabric with 16 layers. For the knife threat, the stab resistance force of STF/UHMWPE composite is close to that of the neat fabric. The energy absorption of STF/fabric composite targets is higher than those of neat fabric and EG/UHMWPE targets for both the spike and knife threats. The STF/fabric composites exhibit better stab resistance and good flexibility compared with neat fabric targets. Therefore, this kind of composite fabric can be used to manufacture the body armor, which is comfortable and has a better stab resistant performance for the users.

ACKNOWLEDGMENTS

This project is supported by the National Natural Science Foundation of China (Grant No. 11172142).

REFERENCES

1. Suemasu, H.; Friedrich, K.; Hou, M. *Compos. Manufact.* **1994**, *5*, 31.

2. Song, Z. Y.; Zhang, C.; Song, M.; Wu, S. Z. *Adv. Mater. Res.* **2011**, *299*, 73.
3. Li, X.; Cao, H.; Gao, S.; Pan, F.; Weng, L.; Song, S.; Huang, Y. *Plast. Rubber Compos.* **2008**, *37*, 223.
4. Decker, M. J.; Halbach, C. J.; Nam, C. H.; Wagner, N. J.; Wetzel, E. D. *Compos. Sci. Technol.* **2007**, *67*, 565.
5. Mayo J. B., Jr.; Wetzel, E. D.; Hosur, M. V.; Jeelani, S. *Int. J. Impact Eng.* **2009**, *36*, 1095.
6. Tan, V.; Tay, T.; Teo, W. *Int. J. Solids Structures* **2005**, *42*, 1561.
7. Termonia, Y. *Int. J. Impact Eng.* **2006**, *32*, 1512.
8. Hu, H.; Wang, J. *Eng. Structures* **2009**, *31*, 1042.
9. Duan, Y.; Keefe, M.; Bogetti, T. A.; Cheeseman, B. A.; Powers, B. *Int. J. Impact Eng.* **2006**, *32*, 1299.
10. Galindo-Rosales, F. J.; Rubio-Hernández, F. J.; Velázquez-Navarro, J. F. *Rheol. Acta* **2009**, *48*, 699.
11. Barnes, H. *J. Rheol.* **1989**, *33*, 329.
12. Huang, K.-Y.; Weng, C.-J.; Huang, L.-T.; Cheng, T.-H.; Wei, Y.; Yeh, J.-M. *Microporous Mesoporous Mater.* **2010**, *131*, 192.
13. Hoffman, R. *J. Colloid. Interface Sci.* **1974**, *46*, 491.
14. Boersma, W. H.; Laven, J.; Stein, H. N. *J. Colloid. Interface Sci.* **1992**, *149*, 10.
15. Wagner, N. J.; Wetzel, E. D. Google Patents, Patent number: US20050557312. **2007**.
16. Farr, R.; Melrose, J.; Ball, R. *Phys. Rev. E* **1997**, *55*, 7203.
17. Phung, T. N.; Brady, J. F.; Bossis, G. *J. Fluid Mech.* **1996**, *313*, 181.
18. Hassan, T. A.; Rangari, V. K.; Jeelani, S. *Ultrason. Sonochem.* **2010**, *17*, 947.
19. Ternik, P.; Marn, J.; Zunic, Z. *J. Non-Newtonian Fluid Mech.* **2006**, *135*, 136.
20. Lee, Y. S.; Wetzel, E. D.; Wagner, N. J. *J. Mater. Sci.* **2003**, *38*, 2825.
21. Hassan, T. A.; Rangari, V. K.; Jeelani, S. *Mater. Sci. Eng.* **2010**, *527*, 2892.
22. Huang, C.-Y.; Wu, J.-Y.; Tsai, C.-S.; Hsieh, K.-H.; Yeh, J.-T.; Chen, K.-N. *Surf. Coat. Technol.*
23. Jin, X.; Wang, W.; Bian, L.; Xiao, C.; Zheng, G.; Zhou, C. *Synth. Met.* **2011**, *161*, 984.
24. dos Santos Alves, A. L.; Cassiano Nascimento, L. F.; Suarez, J. C. M. *Polym. Test.* **2005**, *24*, 104.
25. Lin, C. C.; Lou, C. W.; Hsing, W. H.; Ma, W. H.; Lin, C. M.; Lin, J. H. In Smart Materials; Tunkasiri, T., Ed. *Advan. Mater. Res.* **2008**, *55*, 429–432.
26. Tien, D. T.; Kim, J. S.; Huh, Y. *Fibers Polym.* **2010**, 500.
27. Justice, N. I. o. National Institute of Justice Office of Science and Technology: Washington, DC, Stab Resistance of Personal Body Armor NIJ Standard–0115.00, **2000**.
28. Yang, J.; Chen, J.; Song, J. *Vib. Spectrosc.* **2009**, *50*, 178.